

## X-RAY EMISSION FROM THE SUPER-EARTH HOST GJ 1214

S. LALITHA<sup>1</sup>, K. POPPENHAEGER<sup>2</sup>, K.P. SINGH<sup>1</sup>, S. CZESLA<sup>3</sup> & J.H.M.M. SCHMITT<sup>3</sup>

1. Tata Institute of Fundamental Research, Homi Bhabha road, Mumbai 400005, India

2. Harvard-Smithsonian Center for Astrophysics, 60 Garden St., Cambridge, 02138, MA, USA

3. Hamburger Sternwarte, Universität Hamburg, Gojenbergsweg 112, 21029 Hamburg, Germany.

*The Astrophysical Journal Letters*

### ABSTRACT

Stellar activity can produce large amounts of high-energy radiation, which is absorbed by the planetary atmosphere leading to irradiation-driven mass-loss. We present the detection and an investigation of high-energy emission in a transiting super-Earth host system, GJ 1214, based on an *XMM-Newton* observation. We derive an X-ray luminosity  $L_X = 7.4 \times 10^{25}$  erg s<sup>-1</sup> and a corresponding activity level of  $\log(\frac{L_X}{L_{bol}}) \sim -5.3$ . Further, we determine a coronal temperature of about  $\sim 3.5$  MK, which is typical for coronal emission of moderately active low-mass stars. We estimate that GJ 1214 b evaporates at a rate of  $1.3 \times 10^{10}$  g s<sup>-1</sup> and has lost a total of  $\approx 2.5.6 M_{\oplus}$ .

*Subject headings:* stars: activity – stars: coronae – stars: low-mass, late-type, planetary systems – stars: individual: GJ 1214

### 1. INTRODUCTION

The discovery of the first exoplanet, 51 Peg b, in 1995 (Mayor & Queloz 1995) marked the dawn of the new field called the exoplanetary science. Over  $\sim 1450$  exoplanets have been discovered to date. While initially most of the detected planets were Hot Jupiters, the frontier is inevitably approaching the Earth-mass regime, having already reached a large number of so-called super-Earths, i.e., planets with a mass between 1.9 and 10  $M_{\oplus}$ . Léger et al. (2009) reported the first transiting super-Earth system (CoRoT-7b); soon after, Charbonneau et al. (2009), reported the discovery of the second transiting super-Earth – namely, GJ 1214 b. This planet orbits a nearby (14.5 pc) M4.5-dwarf at a distance of 0.014 AU once every 1.58 days. GJ 1214b, has a radius of 2.68  $R_{\oplus}$  and only  $\sim 6.55$  times the Earth's mass.

The photometric variability detected by the MEarth project suggests the presence of starspots on the surface of GJ 1214. The absence of Hydrogen Balmer  $\alpha$  line emission and the long photometric period, however, indicate a rather mild/low active star (Charbonneau et al. 2009). Nonetheless, GJ 1214 shows flaring activity and even spot crossing signatures in visual transit photometry (see light curves in Kundurthy et al. 2011), clearly demonstrating that it can by no means be completely inactive.

Interestingly, the mass and radius of GJ 1214 b suggest a density of only  $1.9 \pm 0.4$  g cm<sup>3</sup> (Charbonneau et al. 2009), which is inconsistent with it being composed of iron and rock such as the transiting super-Earth CoRoT-7b (Léger et al. 2009). The density of GJ 1214 b is too low for it to be composed of even pure water ice. While the exact composition of the planet, GJ 1214 b, could not yet be uniquely determined by means of theoretical modelling, Rogers & Seager (2010) state that “the planet almost certainly contains a gas component”. In their analysis, the authors consider three different models to explain the interior and the gaseous atmosphere of GJ 1214 b: (1) a mini-Neptune that accreted and maintained a low-mass H/He layer from the primordial

nebula, (2) a superfluid water-world with a sublimating H<sub>2</sub>O envelope, or (3) a rocky planet with a Hydrogen dominated atmosphere formed by recent out-gassing. None of these three scenarios is clearly favoured by their analysis. Detailed calculations of GJ 1214 b's thermal evolution by Nettelmann et al. (2011) favour a metal-enriched envelope. The model that they consider most likely consists of an envelope of 85% water, mixed with Hydrogen and Helium, which resides upon a rocky core, at near-infrared wavelengths. The transmission spectroscopy has, however, revealed a flat atmospheric spectrum (Berta et al. 2012), suggesting either an envelope with large mean molecular weight or the presence of a substantial cloud layer. More detailed observations have shown that the cloud layer interpretation is favoured by the data (Kreidberg et al. 2014).

An important ingredient in atmospheric modelling is the strength of the surrounding high-energy radiation field. Intense high-energy radiation can heat the exosphere of close-in planets to chromospheric temperatures of around 10000 K, which leads to planetary mass loss (Lammer et al. 2003; Yelle 2004; Lecavelier des Etangs et al. 2004; Erkaev et al. 2007). Observations of enhanced hydrogen Ly- $\alpha$  absorption during exoplanetary transits have shown that mass loss rates of atomic hydrogen are of the order of  $\sim 10^9 - 10^{11}$  g s<sup>-1</sup> for the three Hot Jupiters HD 209458 b (Vidal-Madjar et al. 2003; Murray-Clay et al. 2009; Linsky et al. 2010), HD 189733 b (Lecavelier Des Etangs et al. 2010) and WASP-12 b (Fossati et al. 2010; Haswell et al. 2012). Based on theoretical models by Lammer et al. (2003), summarised in Sanz-Forcada et al. (2010), one can also derive an estimate for the total mass loss rate of an exoplanet based on the stellar high-energy irradiation. In the case of an active host star such as CoRoT-2A, the planetary mass-loss rate has been estimated to be as high as  $\sim 4.5 \times 10^{12}$  g s<sup>-1</sup> (Schröter et al. 2011). In the case of CoRoT-7b, which orbits a moderately active star ( $L_X \sim 3 \times 10^{28}$  erg s<sup>-1</sup>, the mass-loss rate has been estimated to about  $\sim 1.3 \times 10^{11}$  g s<sup>-1</sup>, corresponding to an accumulated mass loss of 4-10  $M_{\oplus}$  (Poppenhaeger et al.

TABLE 1  
THE PROPERTIES OF THE GJ 1214 SYSTEM AND THE  
XMM-NEWTON OBSERVATION.

<b>GJ 1214:</b>		
Distance (pc)	14.55±0.13	(a)
Spectral type	M4.5	(b)
<b>GJ 1214 b:</b>		
Mass ( $M_{Jup}$ )	0.0204 ± 0.0031	(b)
Radius ( $R_{Jup}$ )	0.239±0.011	(b)
Orbital period (d)	1.58040482 ± 0.00000024	(c)
Transit mid-point (JD)	2454980.748796± 0.000045	(c)
<b>X-ray data</b>		
Observation start	2013-09-27 18:07:21	
Observation end	013-09-28 03:43:42	
Duration (ks)	34.4	
Primary instrument	XMM-Newton EPIC	
ObsID	0724380101	
Filter	medium	

References. (a) Anglada-Escudé et al. (2013); (b) Charbonneau et al. (2009); (c) Carter et al. (2011).

2012).

The ongoing mass-loss has been observed in a number of hot Jovians, however, the low number, the tiny transit depths, and often large distances of the known super-Earths make the observations in this regime more challenging. Here, we examine the *XMM-Newton* observation of super-Earth host star GJ 1214 and report its X-ray detection with European Photon Imaging Camera (EPIC) detectors at soft X-ray energies. In § 2 we describe the observation and the data analysis, in § 3 we present our results, in § 4 we put GJ 1214b and its host star in context of similar objects and summarise our findings in § 5.

## 2. DATA ANALYSIS

GJ 1214 was observed with *XMM-Newton* for approximately 34 ks (Obs.-ID 0724380101). GJ 1214 b is a transiting planet and therefore, in principle, suited for atmosphere studies. It has recently been shown by Poppenhaeger et al. (2013) that X-ray transits of exoplanets can be much deeper than their optical transits due to extended atmospheric layers. However, our observation did not cover the transit but an orbital phase from 0.33-0.58. An overview of the information on the star-planet system and our observation is given in detail in Table 1.

We only consider data taken with the EPIC, i.e., the two MOS and the PN detector, which were operated in the full frame mode with the medium filter. Those are CCD detectors that are sensitive to X-ray photons with energies between 0.2-15 keV. They provide a moderate energy resolution of  $\sim 100$ eV at energies  $< 2$ keV. Low-mass stars generally display an X-ray spectrum that peaks at energies well below 2 keV, and for the mildly active star like, GJ 1214, no relevant signal was collected at energies above 2 keV at all.

No useful signal from the source is present in the reflection grating spectrometer (RGS) data due to its much lower throughput compared to EPIC. The optical monitor (OM) operated in the fast imaging mode with the UVW1 filter, but GJ 1214 was outside the small observing window of OM. For our analysis of the XMM-Newton data we used the Science Analysis System (SAS) version

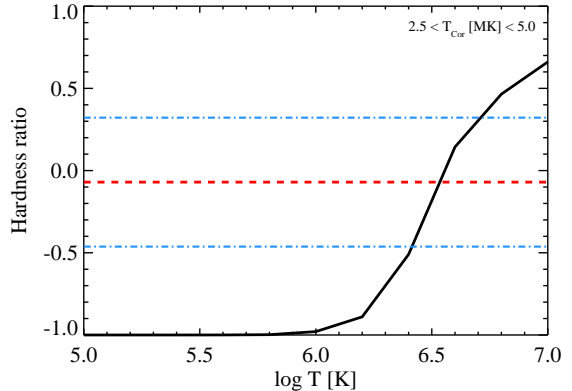


FIG. 1.— Dependence of mean coronal temperature on the expected hardness ratio of *XMM-Newton*'s EPIC detectors (black curve). The measured hardness ratio of GJ 1214 with 68% credibility is plotted as red dashed and blue dotted-dashed lines, respectively.

13.0.0 and followed standard routines for the data reduction.

The merged EPIC data (MOS1+MOS2+PN) shows an X-ray excess at the nominal position of GJ 1214. We extracted the source signal from a circular region with 20'' radius centered on the nominal proper-motion corrected position of GJ 1214 from SIMBAD. The positional error and the offset are about 0.3'' and no other X-ray source is within a radius of 1' around the position of GJ 1214, making the identification unambiguous.

## 3. RESULTS

### 3.1. X-ray luminosity of GJ 1214

The PN detector ran for a total of 32.76 ks, and 97.1 net source counts with significance level of  $5.3 \sigma$  were collected in the 0.2-2 keV band, yielding a PN count rate of  $2.96 \pm 0.32$  counts/ks. The combined two MOS detectors ran for 34.38 ks, collecting 38.1 net source counts with significance level of  $3.4 \sigma$  in the 0.2-2 keV band. The average count rate for a single MOS detector is, therefore,  $0.55 \pm 0.21$  counts/ks.

We estimated the coronal temperature using the hardness ratio from the MOS1, MOS2 and PN source counts. Hardness ratio (HR) for the EPIC was defined as  $HR = \frac{H-S}{H+S}$ , where H is the number of counts between 0.7 and 2.0 keV (hard band) and S is the number of counts between 0.2 and 0.7 keV (soft band). HR determined from the EPIC data is  $0.02 \pm 0.24$ .

We calculated the theoretically predicted hardness ratios, assuming different coronal temperatures. We carried out this modelling using Xspec V 12.8.1 (Arnaud 1996), using a coronal plasma model (APEC model) with a single temperature component whose temperature was varied. Solar elemental abundances from Grevesse & Sauval (1998) were used. In Figure 1, we show the results along with the measurements for GJ 1214. The coronal temperature of GJ 1214 is constrained to lie between 2.5 and 5.0 MK.

Assuming an average coronal temperature of 3.5 MK we calculated the X-ray flux of GJ 1214. Using WebPIMMS, we converted the mean count rate of *XMM-Newton* PN detector into an X-ray flux of  $3.1 \pm 1.9 \times 10^{-15}$

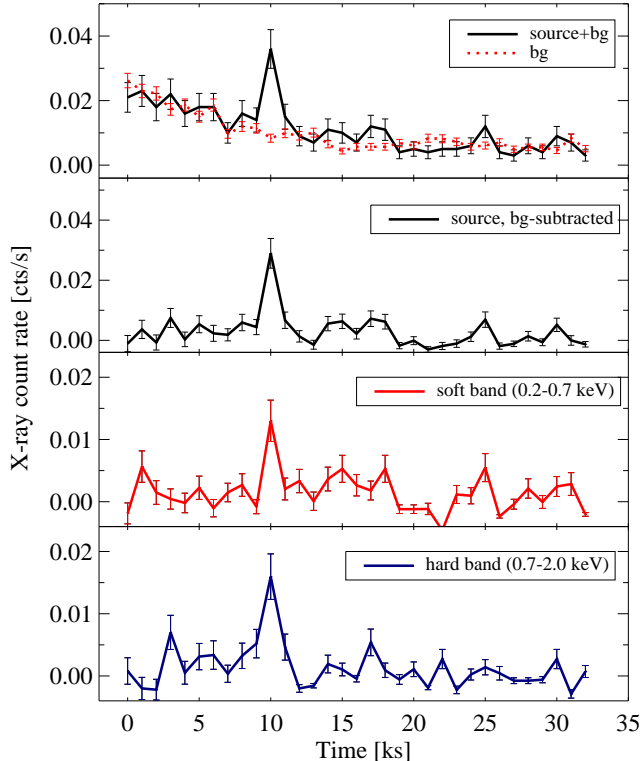


FIG. 2.— (a) Soft X-ray light curve extracted from the source region of GJ 1214 (solid) and the adjacent background region (red dotted), (b) the background-subtracted X-ray light curve of GJ 1214 (0.2-2.0 keV), (c) and (d) show the light curve in the soft band (0.2-0.7 keV) and the hard band (0.7-2 keV), respectively. In panel (b), (c) and (d) a flare-like feature in X-ray flux is observed at  $\sim 10$  ks after the start of the observation.

erg  $\text{s}^{-1} \text{cm}^{-2}$  in the 0.2-2.0 keV energy band. The average signal from the MOS detectors yields a flux estimate of  $3.2 \pm 1.3 \times 10^{-15} \text{ erg s}^{-1} \text{cm}^{-2}$  and is in line with the result from the PN detector. Given a distance of  $\sim 14.55 \pm 0.13 \text{ pc}$ , the observed X-ray flux in PN translates into a luminosity of  $7.8 \pm 4.8 \times 10^{25} \text{ erg s}^{-1}$ . The bolometric luminosity of GJ 1214 can be calculated from  $L_{bol} = 10^{0.4(4.8 - m_v - bc + 5 \log(d) - 5)} L_{\odot}$ , with  $m_v$  denoting the apparent visual magnitude of the star,  $bc$  denoting the bolometric correction,  $d$  the distance in pc and  $L_{\odot}$  the solar bolometric luminosity. Given the apparent V magnitude of 14.67 and K magnitude of 8.78, the bolometric corrections are determined using Worthey & Lee (2011); and the bolometric luminosity is found to be  $1.4 \times 10^{31} \text{ erg s}^{-1}$ . Comparing the X-ray luminosity ( $L_X$ ) to the bolometric luminosity ( $L_{bol}$ ), we determine the ratio of  $\log(\frac{L_X}{L_{bol}}) \approx -5.3$ . The X-ray luminosity as well as the ratio of luminosities point to a mildly active star.

### 3.2. X-ray variability of GJ 1214

We have used the signal from the PN camera, which is more sensitive than the MOS cameras, to extract X-ray light curves of GJ 1214 and for the background region for comparison, using a  $20''$  extraction radius for the source, and a  $50''$  extraction radius for the background. Data were binned every 1000 seconds in energy band of 0.2-2 keV. The resulting light curves for the source and the background are shown in Figure 2 (a).

The background is not constant, it shows a decline over the duration of the observation. We plot the background subtracted X-ray light curve in Fig. 2 (b). After subtraction of the background from the source region signal, we find that GJ 1214 displays a sudden increase in X-ray flux about 10 ks after the start of the observation. This is most likely the signature of a small flare event in GJ 1214's corona. A flare-like signature on GJ 1214 has also been observed in the r-band, where an energy release of  $1.8 \times 10^{28} \text{ erg}$  has been estimated Kundurthy et al. (2011).

To investigate the nature of this flare further, we have split the signal from GJ 1214's PN light curve into two energy bands. In Fig. 2 (c) and Fig. 2 (d), we plot a soft X-ray light curve in 0.2-0.7 keV energy band and a hard X-ray light curve in 0.7-2 keV energy band, respectively. Note that the flare signal is present in both bands with roughly the same amplitude. This implies that the flare did not cause a strong heating of the local corona, because then we would expect to see a stronger signature at harder X-ray energies emitted by the heated plasma.

## 4. DISCUSSION

### 4.1. GJ 1214 b in comparison to the evaporating Jupiter HD 209458 b

X-ray observations show that GJ 1214 b's host star is mildly active, however, the close proximity of the planet to the star places GJ 1214 b in an intense high-energy radiation field. It is, therefore, possible that GJ 1214 b is undergoing atmospheric evaporation. The energy range that is thought to be mainly responsible for atmospheric mass loss is the X-ray and extreme UV range (Lammer et al. 2003).

Sanz-Forcada et al. (2011) computed EUV spectra for several stars using emission measure distribution analyses of X-ray spectra. Later, Claire et al. (2012) and Linsky et al. (2014) compared predicted EUV flux ratios by Sanz-Forcada et al. (2011) for a few stars with the ratios of EUV fluxes measured in different wavelength bands. They found that the values are comparable in all wavelength bands. Hence, we extrapolated the measured X-ray luminosity to the full X-ray and extreme UV (XUV) range using the scaling relation of Sanz-Forcada et al. (2011):

$$\log L_{EUV} = (0.860 \pm 0.073) \log L_X + (4.80 \pm 1.99) \quad (1)$$

$$\log L_{XUV} = \log(L_X + L_{EUV}) \quad (2)$$

For GJ 1214, we find an XUV luminosity of  $\log L_{XUV} = 27.09 \pm 0.02 \text{ erg s}^{-1}$ . To put the irradiation of GJ 1214 b into context, we compare it with the current XUV irradiation of the Earth, and the XUV irradiation of the Hot Jupiter HD 209458 b. In Table 2, we list the various properties of planet hosts and the resultant irradiation levels for the Earth, HD 209458 b and GJ 1214 b. The atmosphere of HD 209458 has been observed in the UV with a very large transit depth (Vidal-Madjar et al. 2003). The interpretations in the literature agree that a very extended atmosphere must be present (Ben-Jaffel 2007; Vidal-Madjar et al. 2003), and active atmospheric escape is likely occurring because the atmosphere is extended beyond the Roche-lobe (Vidal-Madjar et al. 2004), even if the accuracy of velocity measurements of this escaping atmosphere have been

TABLE 2  
PROPERTIES OF THE SUN, HD 209458, AND GJ 1214.

Parameters	Sun	HD 209458	GJ 1214
Sp. type	G2V	G0V	M4.5
$\log L_X$	27.0	<26.12	25.87
$\log \frac{L_X}{L_{bol}}$	$\approx -6.6$	<-7.6	-5.3
$a_P$ (AU)	1.00	0.047	0.014
$P_{orb}$ (d)	365	3.52	1.58
$M_P$ ( $M_E$ )	1.00	219	6.47
$F_X$ [ $erg\ s^{-1}\ cm^{-2}$ ] at planet orbit	0.35	<21.4	135.6
$F_{XUV}$ [ $erg\ s^{-1}\ cm^{-2}$ ] at planet orbit	4.1	<312	2150

debated (Ben-Jaffel 2008). HD 209458 has been observed in X-rays, but not been detected, though, a firm upper limit of  $\log L_X < 26.12\ erg\ s^{-1}$  has been established (Sanz-Forcada et al. 2010).

In comparison to HD 209458 b the XUV flux at the planetary orbit of GJ 1214 b is substantially larger, by about an order of magnitude (Table 2). We also show the respective values for the Earth, using a solar X-ray luminosity of  $\log L_X = 27\ erg\ s^{-1}$  (Judge et al. 2003).

The strong high-energy irradiation of GJ 1214 b suggests that the atmosphere of this planet may be evaporating. We proceed by estimating how much mass the planet may be losing, given analytical theoretical models.

#### 4.2. Estimated evaporation of GJ 1214b

In the picture of energy-limited hydrodynamic mass-loss (Watson et al. 1981; Lammer et al. 2003; Sanz-Forcada et al. 2010), the mass-loss rate,  $\dot{M}$ , amounts to:

$$\dot{M} = \frac{\pi R_p^3 \epsilon F_{XUV}}{G K M_p}, \quad (3)$$

where  $R_p$  is the planetary radius,  $F_{XUV}$  is the incident X-ray and EUV-flux,  $\epsilon = 0.4$  is the heating efficiency as suggested by Valencia et al. (2010),  $G$  is the gravitational constant,  $M_p$  the mass of the planet, and  $K$  is a parameter accounting for Roche-lobe filling, which we assume to be unity here. According to Valencia et al. (2010), the above expression remains valid for strongly irradiated rocky planets, because the atmosphere may be replenished by sublimation faster than it erodes. Therefore, assuming a density of  $\approx 1.9\ g\ cm^{-3}$  (Charbonneau et al. 2009) and substituting the XUV luminosity of  $\log L_{XUV} \approx 27.09\ erg\ s^{-1}$  into Eq. 3, yields an estimate of  $1.3 \times 10^{10}\ g\ s^{-1}$  for mass-loss rate of GJ 1214 b.

The high-energy emission for super-Earth host star has been measured, so far, for only CoRoT-7, a subsolar mass star with spectral type G8-K0 (Poppenhaeger et al. 2012). They, estimated a mass loss rate of  $0.5\text{--}1.0 \times 10^{11}\ g\ s^{-1}$  for CoRoT-7b, comparable within an order of magnitude to the value obtained here.

The stellar X-ray and UV emission is not constant over time. Young stars usually display much higher X-ray luminosities than older stars. Scaling relations for X-ray luminosity and age have been given by several authors,

for example Ribas et al. (2005); Lammer et al. (2009). We assume here that the X-ray luminosity increases with age by a factor  $(\frac{\tau}{\tau_*})^{1.23}$ , where  $\tau$  is the young stellar age

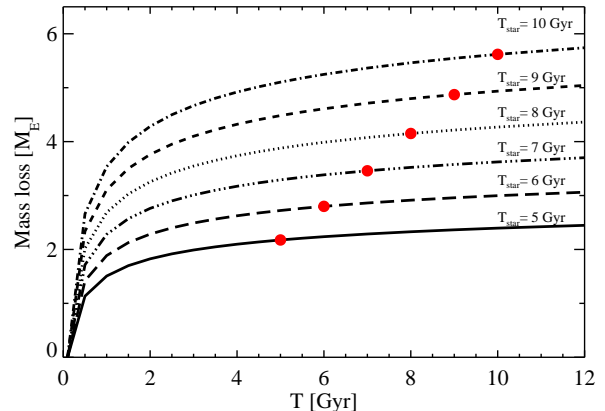


FIG. 3.— Evolution of the total planetary mass-loss for the current X-ray luminosity. The filled points indicate the current age.

when the stellar activity remains at a constant level (0.1 Gyr) and  $\tau_*$  is the current stellar age in Gyr (Ribas et al. 2005).

Estimating the current age of the host star GJ 1214 is not an easy task. Typical age-activity relationships display substantial scatter, especially for older stars (Mamajek & Hillenbrand 2008). Poppenhaeger & Wolk (2014) have recently compiled X-ray luminosities of old disk and halo dwarfs of different spectral types in order to test for exoplanetary influences on stellar rotation and activity. They give a typical X-ray luminosity range of  $\log L_X = 25.76$  to  $27.21\ erg\ s^{-1}$  for old disk/halo M dwarfs. GJ 1214 falls well into this range with its X-ray luminosity of  $\log L_X = 25.87\ erg\ s^{-1}$ . An age of 5-10 Gyr therefore seems likely for this star. Inserting the time variable XUV flux into Eq. 3 and integrating over stellar ages of 5-10 Gyr, we plot the mass loss history of GJ 1214 b in Figure 3; each curve represents a different age of GJ 1214 system. Considering the large uncertainty in the age of GJ 1214, we estimate a total mass loss of 2-5.6  $M_\oplus$ .

## 5. SUMMARY

We report X-ray emission from a nearby super-Earth host, GJ 1214. In the quiescent state GJ 1214 is detected at soft X-ray energies (0.2-2.0 keV) with an X-ray luminosity of  $\sim 7.4 \times 10^{25}\ erg\ s^{-1}$ . This leads to an X-ray activity level of  $\log \frac{L_X}{L_{bol}} \approx -5.3$ , combined with a likely coronal temperature  $\approx 3.5\ MK$ , points to a mildly active star. We notice a small flare-like signature in the X-ray light curve, however, we found no evidence of this event triggering any strong heating of the local corona.

Extrapolation of the X-ray luminosity to extreme UV range leads to XUV flux of  $2150\ erg\ s^{-1}\ cm^{-2}$  at the planetary orbit and a mass loss rate of  $1.3 \times 10^{10}\ g\ s^{-1}$  for GJ 1214 b. Integration of the stellar activity history, leads to a mass loss of  $\approx 2\text{--}5.6\ M_\oplus$  over the lifetime of the planet.

## REFERENCES

- Ben-Jaffel, L. 2007, *ApJ*, 671, L61  
Ben-Jaffel, L. 2008, *ApJ*, 688, 1352  
Berta, Z. K., et al. 2012, *ApJ*, 747, 35  
Carter, J. A., Winn, J. N., Holman, M. J., Fabrycky, D., Berta, Z. K., Burke, C. J., & Nutzman, P. 2011, *ApJ*, 730, 82  
Charbonneau, D., et al. 2009, *Nature*, 462, 891  
Claire, M. W., Sheets, J., Cohen, M., Ribas, I., Meadows, V. S., & Catling, D. C. 2012, *ApJ*, 757, 95  
Erkaev, N. V., Kulikov, Y. N., Lammer, H., Selsis, F., Langmayr, D., Jaritz, G. F., & Biernat, H. K. 2007, *A&A*, 472, 329  
Fossati, L., et al. 2010, *ApJ*, 714, L222  
Grevesse, N., & Sauval, A. J. 1998, *Space Sci. Rev.*, 85, 161  
Haswell, C. A., et al. 2012, *ApJ*, 760, 79  
Judge, P. G., Solomon, S. C., & Ayres, T. R. 2003, *ApJ*, 593, 534  
Kreidberg, L., et al. 2014, *Nature*, 505, 69  
Kundurthy, P., Agol, E., Becker, A. C., Barnes, R., Williams, B., & Mukadam, A. 2011, *ApJ*, 731, 123  
Lammer, H., et al. 2009, *A&A*, 506, 399  
Lammer, H., Selsis, F., Ribas, I., Guinan, E. F., Bauer, S. J., & Weiss, W. W. 2003, *ApJ*, 598, L121  
Lecavelier Des Etangs, A., et al. 2010, *A&A*, 514, A72  
Lecavelier des Etangs, A., Vidal-Madjar, A., McConnell, J. C., & Hébrard, G. 2004, *A&A*, 418, L1  
Léger et al., a., A. et. 2009, *A&A*, 506, 287  
Linsky, J. L., Fontenla, J., & France, K. 2014, *ApJ*, 780, 61  
Linsky, J. L., Yang, H., France, K., Froning, C. S., Green, J. C., Stocke, J. T., & Osterman, S. N. 2010, *ApJ*, 717, 1291  
Mamajek, E. E., & Hillenbrand, L. A. 2008, *ApJ*, 687, 1264  
Mayor, M., & Queloz, D. 1995, *Nature*, 378, 355  
Murray-Clay, R. A., Chiang, E. I., & Murray, N. 2009, *ApJ*, 693, 23  
Nettelmann, N., Fortney, J. J., Kramm, U., & Redmer, R. 2011, *ApJ*, 733, 2  
Poppenhaeger, K., Czesla, S., Schröter, S., Lalitha, S., Kashyap, V., & Schmitt, J. H. M. M. 2012, *A&A*, 541, A26  
Poppenhaeger, K., Schmitt, J. H. M. M., & Wolk, S. J. 2013, *ApJ*, 773, 62  
Poppenhaeger, K., & Wolk, S. J. 2014, *A&A*, 565, L1  
Ribas, I., Guinan, E. F., Güdel, M., & Audard, M. 2005, *ApJ*, 622, 680  
Rogers, L. A., & Seager, S. 2010, *ApJ*, 716, 1208  
Sanz-Forcada, J., Micela, G., Ribas, I., Pollock, A. M. T., Eiroa, C., Velasco, A., Solano, E., & García-Álvarez, D. 2011, *A&A*, 532, A6  
Sanz-Forcada, J., Ribas, I., Micela, G., Pollock, A. M. T., García-Álvarez, D., Solano, E., & Eiroa, C. 2010, *A&A*, 511, L8  
Schröter, S., Czesla, S., Wolter, U., Müller, H. M., Huber, K. F., & Schmitt, J. H. M. M. 2011, *A&A*, 532, A3  
Valencia, D., Ikoma, M., Guillot, T., & Nettelmann, N. 2010, *A&A*, 516, A20  
Vidal-Madjar, A., et al. 2004, *ApJ*, 604, L69  
Vidal-Madjar, A., Lecavelier des Etangs, A., Désert, J.-M., Ballester, G. E., Ferlet, R., Hébrard, G., & Mayor, M. 2003, *Nature*, 422, 143  
Watson, A. J., Donahue, T. M., & Walker, J. C. G. 1981, *Icarus*, 48, 150  
Worthey, G., & Lee, H.-c. 2011, *ApJS*, 193, 1  
Yelle, R. V. 2004, *Icarus*, 170, 167